Supplemental Figure Legends

Figure S1. Characterization of the OE in *OAZ*$^{-/-}$ mice

(A) BrdU labeling is shown in low magnification. There is no obvious difference in BrdU labeling across dorsal-ventral zones in the OE. (B) GAP43 *in situ* hybridization in control and *OAZ*$^{-/-}$ mice shown in low magnification. (C) NeuroD1 *in situ* hybridization shows similar pattern in control and *OAZ*$^{-/-}$ mice.

Figure S2. *OAZ* homolog *Evi3* is expressed in the olfactory epithelium. (A) RT-PCR from OE RNA using two primer sets specific for mouse *Evi3* (see supplemental methods). The expected products are 566bp (Primer Pair #1) and 527bp for Primer Pair #2. PCR reactions were performed on templates prepared in the presence (+RT) or absence (-RT) of reverse transcriptase to control for genomic contamination. (B, C) *In situ* hybridization with *Evi3* antisense and sense probes (nucleotides 1 to 1172 of BC021376).

Figure S3. Defects in ORN projection in *OAZ*$^{-/-}$ mice

(A-D) Whole-mount dorsal view of ORN projection visualized by *O/E3*-tauGFP reporter. In *OAZ*$^{-/-}$ mice, ORN axons fail to innervate the caudal OB (indicated by an arrows). (E-N) A series of anterior to posterior coronal sections through the OB in control and *OAZ*$^{-/-}$ mice. The dorsal OB surface is devoid of olfactory nerves and glomeruli. Instead, extra glomeruli accumulate at the ventral surface (indicated by "*").

Figure S4. *In situ* hybridization of OR genes in $O/E3^{OAZ/+}$ mice and controls

(A-C) Hybridization with M71/M72, M4 and I7 probes revealed that each of the OR genes are expressed in relatively few cells at levels that can be detected by *in situ* methods. Specifically, OR genes detected by specific OR-reporter tagging were not visible in the immature cells in $O/E3^{OAZ/+}$ mice.

Figure S5. ORN projection defects in $O/E3^{OAZ/+}$ mice

(A, B) OMP staining in OB shows the lack of glomeurli in $O/E3^{OAZ/+}$ mice. (C, D) GAP43 staining in wild-type OB shows a strong staining in the olfactory nerve layer and weak staining in the glomeurlar layer. In $O/E3^{OAZ/+}$ mice, the glomeruli were absent. (E, F) Merged images of OMP/GAP43 double-labeling suggest that GAP43-expressing axons failed to innervate the OB.

Figure S6. Whole-mount X-gal staining of *P2-IRES-taulacZ* reporter in $O/E3^{OAZ/+}$ mice and controls at around P90. The convergence of P2-labeled axons to the ventral surface of the bulb is significantly perturbed in $O/E3^{OAZ/+}$ mice. Labeled axons extend to a broad region of the OB.

Figure S7. Role of OAZ in olfactory development

In OAZ knockout mice, ORN axons fail to project to the dorsal caudal OB, but accumulate at the ventral OB. This axon projection defects could account for the increased apoptosis and decreased mature cells in the OE. The presence of the OAZ

homolog, Evi3, in the OE may prevent a complete analysis of the OAZ loss-of-function phenotype. In OAZ knock-in mice, introduced OAZ expression in late ORN development decreases mature marker expression, and reactivates immature marker expression. The arrest of maturation phenotype is accompanied by altered OR gene expression and defects in axonal projection. This phenotype is consistent with the proposed role of OAZ as an inhibitor of the O/E family transcription factors, but also implicates involvement of additional pathways.

Supplemental Methods

***OAZ-lacZ* gene-trap clone XB409**. The ES cell clone was obtained from Baygenomics (www. baygenomics. ucsf.edu), the site of genomic insertion and fusion of *OAZ* gene with lacZ was confirmed by RT-PCR from ES RNA, and injected into C57BL/6 balstocysts. The genomic insertion site was mapped by genomic southern blot and confirmed by sequencing. After germ line transmission, the heterozygous $OAZ^{lacZ/+}$ mice were backcrossed with C57BL/6, and the line was maintained either by heterozygous intercrosses or by heterozygous backcrossing to C57BL/6 mice. Homozygous $OAZ^{lacZ/lacZ}$ pups were born, but died within one day of birth, indicating the insertion also disrupts OAZ function.

***OAZ-null* allele**. The *OAZ* large exon 4 was targeted by homologous recombination. An *IRES-YFP-polyA* cassette followed by the *LoxP-TK(Δ)-Neo-LoxP (LTNL)* selection cassette was inserted at 55 nucleotides downstream of exon 4 splicing acceptor and eliminated the remainder of OAZ open reading frame (1159 of 1271 amino acids). The truncated OAZ protein, if stable, would contain a single Zinc-finger but lacks all the

known DNA binding and protein binding domains of OAZ. The requirement for multiple Zinc fingers for DNA binding in most other proteins suggests that this allele would be a functional null. Homologous integrants were identified by Southern blot and correctly targeted ES cells were injected into C57BL/6 blastocysts. The F1 heterozygous mice were mated with Cre-expressing transgenic mice to remove the *LTNL* cassette, and the line was maintained by heterozygous intercrosses. Homozygous $OAZ^{-/-}$ mice were smaller, ataxic and died at the time of weaning. Examination of $OAZ^{-/-}$ brain showed defects in cerebellar development (Cheng and Reed, 2007).

RT-PCR

Total RNA from mouse olfactory tissue was extracted by Trizol® reagent (invitrogen). First strand cDNA was synthesized using Superscript reverse transcriptase and oligo-dT. Primer pair #1 (forward primer, 5'-TTTGAGCACCAGATAGACAGACTCC -3'; reverse primer, 5'-CCGCAGGGTAAACATTGAGAGC-3') and primer pair #2 (forward primer, 5'-GGATGGAGGACTGGAAGATGAAG-3'; reverse primer, 5'-TGTAGGTGACTTTCGCCTGCTTAC-3') was used to amplify Evi3 message.

Supplemental figure 1

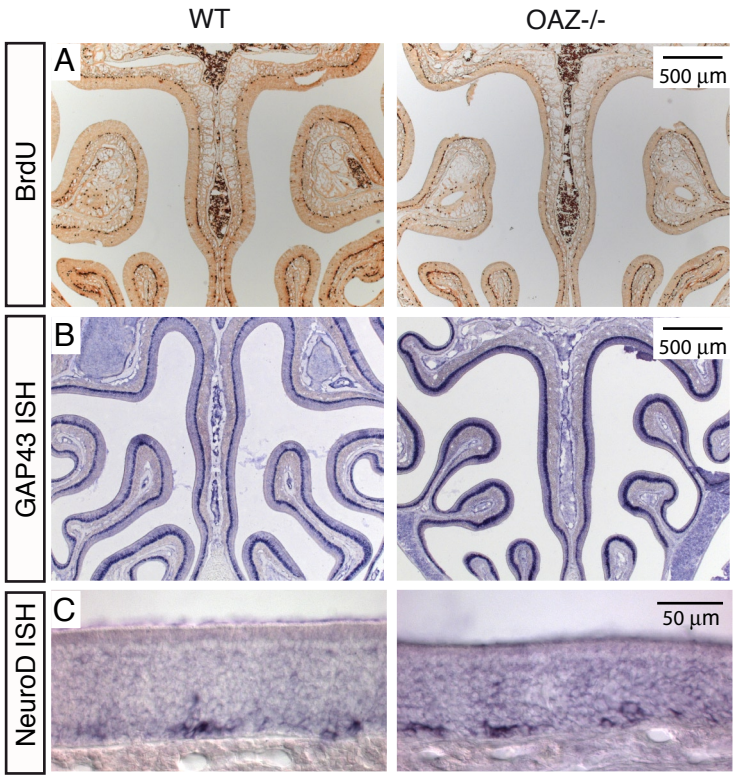

Supplemental figure 2

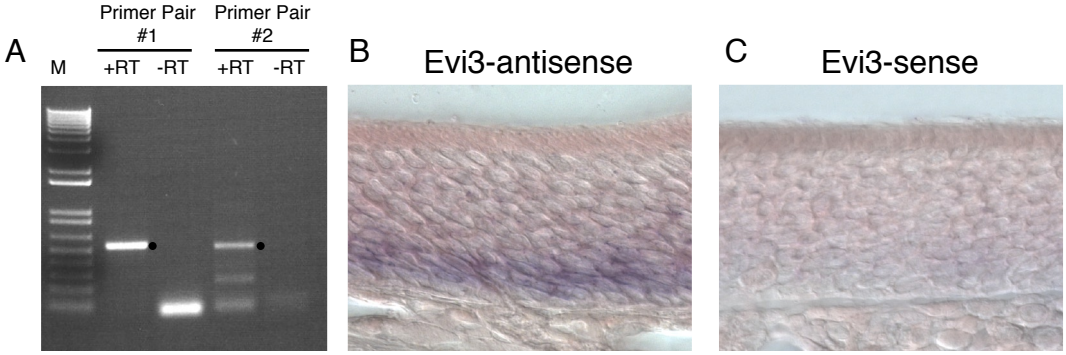

RT-PCR

In situ hybridization

Supplemental figure 3

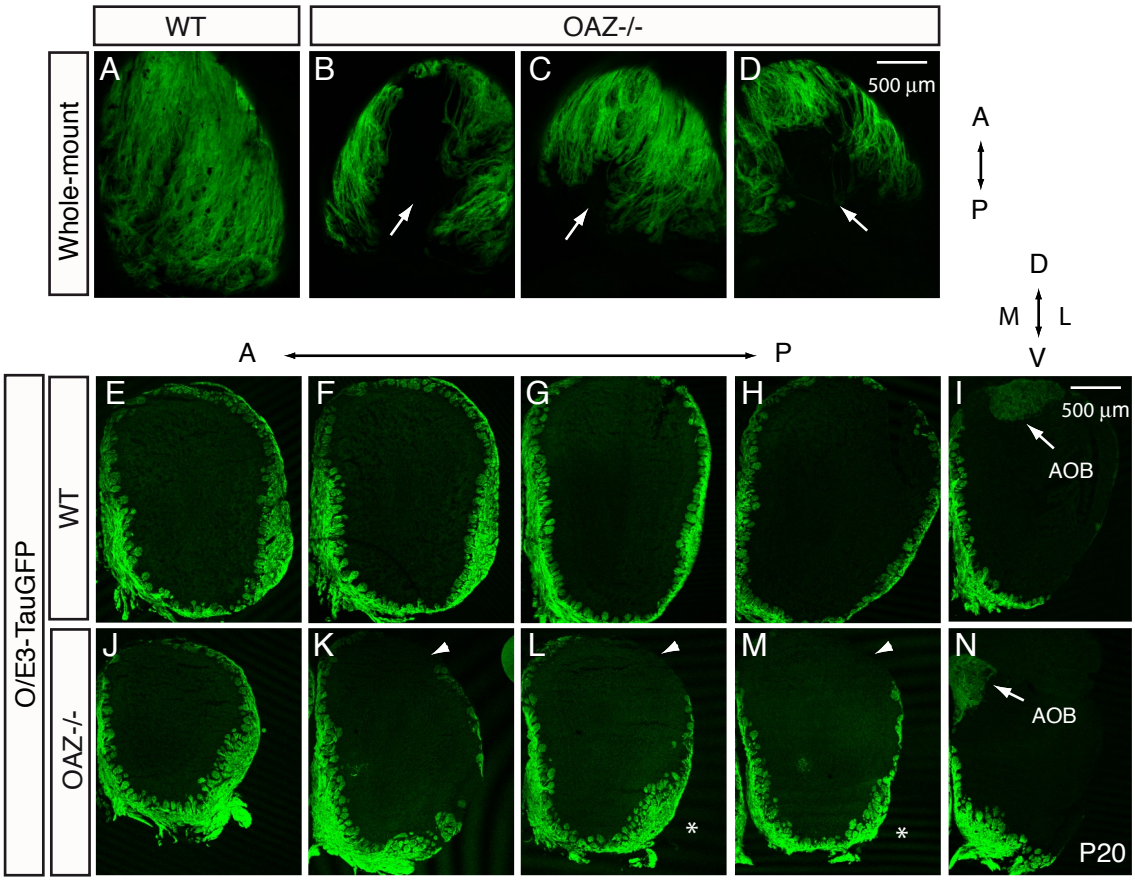

Supplemental figure 4

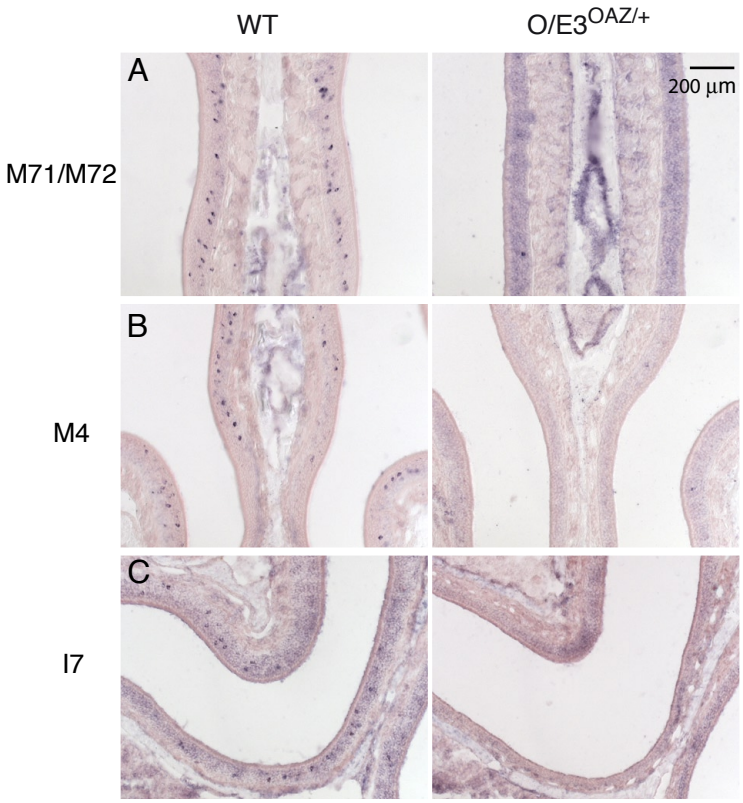

Supplemental figure 5

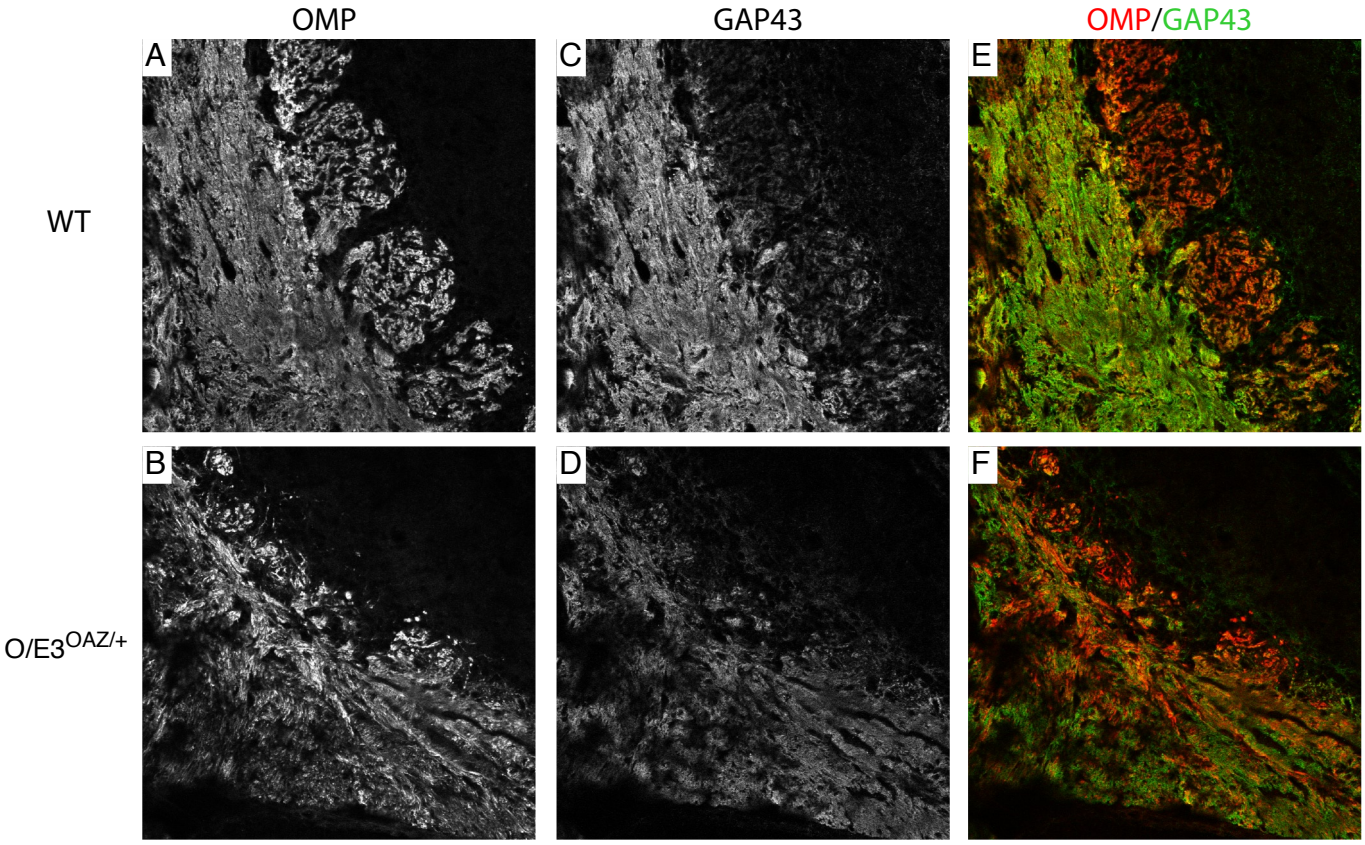

Supplemental figure 6

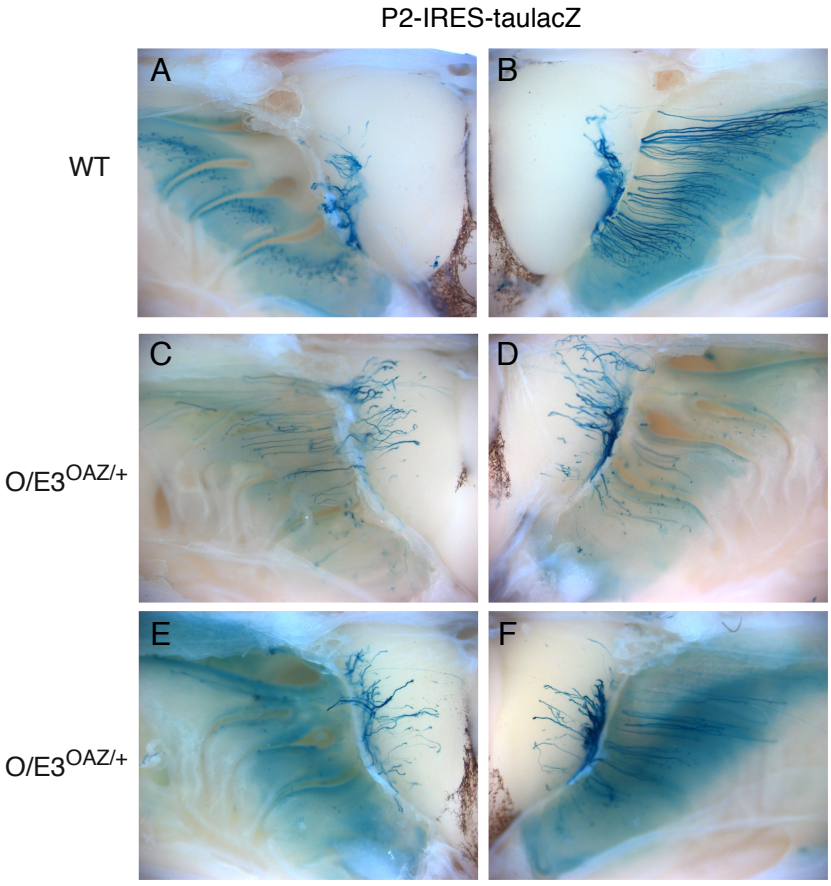

Supplemental figure 7